Dynamics of the excitation of an upper hybrid wave by a rippled laser beam in magnetoplasma

Gunjan Purohit, P. K. Chauhan, and R. P. Sharma

Citation: Physics of Plasmas 15, 052101 (2008); doi: 10.1063/1.2908353
View online: http://dx.doi.org/10.1063/1.2908353
View Table of Contents: http://scitation.aip.org/content/aip/journal/pop/15/5?ver=pdfcov
Published by the AIP Publishing

Dynamics of the excitation of an upper hybrid wave by a rippled laser beam in magnetoplasma

Gunjan Purohit,[1] P. K. Chauhan,[2,a)] and R. P. Sharma[2]
[1]Department of Physics, HNB Garhwal University, Srinagar (Garhwal), Uttarakhand-246174, India
[2]Centre for Energy Studies, Indian Institute of Technology Delhi, New Delhi-110016, India

(Received 4 December 2007; accepted 21 March 2008; published online 1 May 2008)

This paper presents the effects of a laser spike (superimposed on an intense laser beam) and a static magnetic field on the excitation of the upper hybrid wave (UHW) in a hot collisionless magnetoplasma, taking into account the relativistic nonlinearity. The laser beam is propagating perpendicular to the static magnetic field and has its electric vector polarized along the direction of the static magnetic field (ordinary mode). Analytical expressions for the growth rate of the ripple, the beam width of the rippled laser beam, and the UHW have been obtained. It is found that the coupling among the main laser beam, ripple, and UHW is strong. The ripple gets focused when the initial power of the laser beam is greater than the critical power for focusing. It has been shown that the presence of a laser spike affects significantly the growth rate and the dynamics of the UHW. In addition, it has been seen that the effect of changing the strength of the static magnetic field on the nonlinear coupling and on the dynamics of the excitation of the UHW is significant. The results are presented for typical laser plasma parameters. © *2008 American Institute of Physics*.
[DOI: 10.1063/1.2908353]

I. INTRODUCTION

An efficient coupling of a high-power laser beam with plasma is a topic of current research interest in many areas such as laser induced fusion[1] and particle acceleration.[2,3] Due to the availability of lasers capable of delivering high power (10^{19}–10^{21} W/cm^2), its interaction with plasmas becomes a most interesting and important nonlinear problem. At such intensities, the response of plasma free electrons is fully relativistic (electrons swing in the laser pulse) and highly nonlinear. In the laser plasma coupling process, when a high-power laser beam interacts with the plasma, various parametric instabilities (such as self-focusing, filamentation, stimulated Raman scattering, stimulated Brillouin scattering, two plasmon decay, etc.) take place, and due to this, the energy of the high-power laser beam is not efficiently coupled with plasma.[1,4] Therefore, the study of these nonlinear phenomena at high-power laser flux is being studied theoretically and experimentally.

Filamentation of laser beams in plasma is one of the parametric instabilities that led to degrade performance of inertial confinement fusion targets. The origin of filamentation instability may be attributed to small-scale intensity spikes associated with the main beam. In recent years, new laser beam smoothing techniques such as random phase plate[5] (RPP), smoothing by spectral dispersion[6] (SSD), and induced spatial incoherence[7] (ISI) have been used for controlling natural intensity nonuniformities in laser beams. This in turn improves the efficiency of laser energy coupling to the plasma and uniformity of fuel compression in inertial confinement fusion targets. A lot of theoretical and experimental work has been reported on filamentation instability in recent years.[8–12] Sartang *et al.*[13] followed the evolution of the paraxial wave equation (nonlinear Schrödinger equation) in the presence of a ponderomotive type of nonlinearity; they observed filaments combining and splitting in different circumstances. Wilks *et al.*[14] looked at cases of strong self-focusing followed by spreading and beam breakup. A very comprehensive paper by Schmitt[15] includes analytic and numerical treatment of filamentation, the breakup of single beams into multiple filaments, and the statistical effects of changing laser beam patterns as a function of time. Ren *et al.*[16] used a fully three-dimensional particle-in-cell (PIC) model of laser light in a plasma to demonstrate the mutual attraction of two skew beams that results in the light filaments twisting and forming a braided pattern. However, at high laser powers, the dynamics of filamentation and its effect on laser propagation are poorly understood.

Most of the earlier studies assumed that the plasma was unmagnetized. There has been much less study of the laser plasma interactions in magnetized plasma. In the presence of a magnetic field, various waves are excited in plasma when they interact with strong radiation. Magnetic fields play an important role in many interesting problems such as excitation of an upper hybrid wave to heat the plasma near upper hybrid frequency, radiation from Cerenkov wakes, particle acceleration, and they could play a role in the fast ignitor concept in inertial confinement fusion (ICF), in which either self-generated or external magnetic fields could be important. The coupling of an intense radiation field and a plasma is thus of great interest in the case of magnetized plasma. Moreover, the nature and polarization of the incident laser beam also play an important role during laser plasma interaction in magnetized plasma. The ordinary wave remains unaffected by the presence of external magnetic field, and its dispersion relation remains the same as it has in unmagnetized plasma. While in the case of an extraordinary wave the

a)Electronic mail: praishi_nbd@yahoo.com.

electromagnetic (EM) wave tends to be elliptically polarized instead of plane polarized and it become partly longitudinal and partly transverse in nature, its dispersion relation also gets modified with two cutoff frequencies in magnetized plasma.

Significant heating of plasmas by high-power lasers and successful operation of the laser pellet implosion schemes depend crucially on good coupling of the laser power to the plasma.[17] When the plasma is heated by a relativistic laser beam, it may excite the natural modes of vibration of the plasma, i.e., the electron plasma wave and ion waves. This electron plasma wave can have a very high phase velocity (of the order of the velocity of light), and so can produce very energetic electrons when it damps. Such electrons can preheat the fuel in laser fusion applications.[1] The temperature is of interest for controlled fusion; plasma is heated by exciting the natural modes of the plasma (upper hybrid wave) by a laser. The excited upper hybrid wave after Landau damping transfers its energy to the plasma particles and leads to enhanced heating of the plasma. The background electron concentration is modified as a result of the finite ponderomotive force and relativistic mass correction. The amplitude of the natural modes, which depends on the background concentration, is nonlinearly coupled with the laser beam.

Heating of plasmas by exciting the upper hybrid waves and other waves generated during laser plasma has been investigated and reported by many authors.[18–26] In the presence of static magnetic field, the excitation is determined in the direction of propagation of the pump laser beam with respect to the static magnetic field, by the polarization of the pump laser beam, and by the nature of the electrostatic mode being excited by the laser beam. Sodha *et al.*[27] reported the excitation of an upper hybrid wave by a Gaussian laser beam in ordinary mode, taking into account the ponderomotive nonlinearity, and they concluded that the focusing nature of the upper hybrid wave is highly dependent on the initial power of the laser and the strength of the magnetic field. Grebogi and Liu[28] studied the effects of a self-generated magnetic field in laser produced plasma on the parametric decay of an extraordinary wave into two upper hybrid plasmons. They concluded that the two-plasmon decay growth rate decreases with increasing magnetic field. Krasovitskii *et al.*[24,25] also reported the heating of plasma particles by upper hybrid waves (UHW), and waves generated during the laser plasma interaction, considering the laser beam as an extraordinary mode and propagating across the applied magnetic field. However, these studies used a spatially smooth laser beam, which is not realistic. In a realistic case, the laser beam is not perfectly spatially smooth; rather, it has multiple ripples of different intensities superimposed on it. The effect of these ripples on the excitation of an upper hybrid wave has not been studied so far.

The outline of the paper is as follows. In Sec. II, we derive the expression for the growth rate and relativistic self-focusing of the rippled laser beam in a hot collisionless magnetoplasma. An expression for the density perturbation associated with the excited upper hybrid wave in the presence of a rippled laser beam has been studied in Sec. III. Section IV presents a brief discussion of the results and conclusions.

II. PROPAGATION OF A RELATIVISTIC LASER BEAM IN MAGNETOPLASMA AND GROWTH OF A LASER SPIKE

Consider a high-power laser beam of frequency ω_0 and wave number k_0, which propagates in a hot collisionless magnetoplasma along the x direction; the electric vector of the beam is parallel to the static magnetic field (B_0) along the z direction. The intensity distribution of the beam at ($x=0$) is given by

$$E_0 \cdot E_0^*\big|_{x=0} = E_{00}^2 e^{-(r^2/r_0^2)}, \tag{1}$$

where r_0 is the initial beam width, $r(r^2=y^2+z^2)$ is the radial coordinate of cylindrical coordinate system, and E is the axial amplitude.

Let a perturbation be superimposed on the main beam. The initial intensity distribution of the ripple on the main beam may be expressed as[29]

$$E_1 \cdot E_1^*\big|_{x=0} = E_{100}^2 \left(\frac{r}{r_{10}}\right)^{2n} e^{-(r^2/r_{10}^2)}, \tag{2}$$

where n is a positive number and r_{100} is the width of the ripple. By changing the value of n, the position of the ripple changes. The total electric vector of the beam is

$$E = E_0 + E_1. \tag{3}$$

The wave equation governing the electric vector of a beam in plasma with dielectric constant ε can be written as

$$\nabla^2 E - \nabla(\nabla \cdot E) + \left(\frac{\omega_0^2}{c^2}\right)\varepsilon E = 0, \tag{4}$$

where $\varepsilon=\varepsilon_0+\phi(E\cdot E^*)$ ε_0 and $\phi(E\cdot E^*)$ are the linear and nonlinear parts of the dielectric constant, ω_0 is the angular frequency of the wave, and c is the speed of light in vacuum, respectively. The dielectric constant of the plasma is given by

$$\varepsilon_0 = 1 - \frac{\omega_{p0}^2}{\omega_0^2}, \tag{5}$$

where $\omega_{p0}^2=4\pi n_0 e^2/m_0$ is the electron plasma frequency in the absence of the laser beam, where n_e is the density of plasma electrons, e and m_0 are the charge and rest mass of electron, respectively. The relativistic general expression for the plasma frequency is

$$\omega_p^2 = \frac{\omega_{p0}^2}{\gamma_0}, \tag{6}$$

where γ_0 is the relativistic factor given by

$$\gamma_0 = \left(1 + \frac{e^2}{m_0^2\omega_0^2 c^2} E \cdot E^*\right)^{1/2}. \tag{7}$$

The nonlinear relativistic part of the dielectric constant can be expressed as

$$\phi(E\cdot E^*) = \left(\frac{\omega_{p0}^2}{\omega_0^2}\right)\left[1-\frac{1}{\gamma_0}\right] = \left(\frac{\omega_{p0}^2}{\omega_0^2}\right)\left[1-\left(1+\alpha E\cdot E^*\right)^{-1/2}\right], \quad (8)$$

where $\alpha = e^2/m_0^2\omega_0^2c^2$. To solve Eq. (4), the Wentzel–Kramers–Brillouin (WKB) approximation has been used. In the WKB approximation, the second term $\nabla(\nabla.E)$ of Eq. (4) has been neglected, which is justified when $c^2/\omega_0^2|1/\varepsilon\nabla^2 \ln\varepsilon| \leq 1$. The electric vector of the main beam (E_0) can be expressed as

$$\nabla^2 E_0 + \frac{\omega_0^2}{c^2}\varepsilon(E_0\cdot E_0^*)E_0 = 0. \quad (9)$$

In the presence of the modified background electron concentration due to relativistic nonlinearity, the intensity distribution of the beam inside the plasma can be obtained by using the WKB and paraxial ray approximations. Following Akhmanov *et al.*[30] and Sodha *et al.*,[31] the solution for E can be written as

$$E = A_0(x,y,z)e^{i[\omega_0 t - k_0(x+S_0)]},$$

where

$$A_0^2 = \left(\frac{E_{00}^2}{f_0^2}\right)e^{(-r^2/r_0^2 f_0^2)},$$

$$S_0 = \left(\frac{r^2}{2}\right)\beta_0(x) + \phi_0(x), \quad (10)$$

$$\beta_0(x) = \frac{1}{f_0}\frac{df_0}{dx}, \quad k_0 = \frac{\omega_0}{c}\varepsilon_0^{1/2},$$

where $\phi_0(x)$ is a constant independent of r and is not needed in the subsequent analysis and f_0 is the dimensionless beam width parameter given by[32]

$$\frac{d^2 f_0}{dx^2} = \frac{c^2}{\omega_0^2 r_0^4 \varepsilon_0 f_0^3} - \frac{1}{2r_0^2\varepsilon_0 f_0^3}\left[\left(\frac{\omega_{p0}^2}{\omega_0^2}\alpha E_0^2\right)\times\left(1+\frac{\alpha E_0^2}{f_0^2}\right)^{-3/2}\right]. \quad (11)$$

The initial conditions on f_0 for a plane wavefront are $df_0/dx=0$ and $f_0=1$ at $x=0$. Equation (11) governs the variation of the beam width parameter f_0 with distance of propagation. The first term on the right-hand side (RHS) corresponds to diffraction divergence of the beam. This equation provides the beam width inside the plasma at any axial distance for any arbitrary cross section of incident beam. The beam becomes self-focused if the initial power is between the two critical powers.

The electric vector of the ripple (E_1) satisfies the following equation [when the second term in Eq. (4) is neglected]:

$$\nabla^2 E_1 + \frac{\omega_0^2}{c^2}\varepsilon(E\cdot E^*)E_1 + \frac{\omega_0^2}{c^2}[\phi(E\cdot E^*) - \phi(E_0\cdot E_0^*)]E_0 = 0. \quad (12)$$

To obtain the solution of Eq. (12), we express

$$E_1 = A_1(x,y,z)\exp(-ik_0 x), \quad (13)$$

where A_1 is a complex function of space. Substituting Eq. (13) into Eq. (12), we get the following equation within the WKB approximation:

$$-2ik_0\frac{\partial A_1}{\partial x} + \left(\frac{\partial^2 A_1}{\partial y^2}+\frac{\partial^2 A_1}{\partial z^2}\right) + \frac{\omega_0^2}{c^2}\phi(E\cdot E^*)A_1 + \frac{\omega_0^2}{c^2}[\phi(E\cdot E^*) - \phi(E_0\cdot E_0^*)]A_0 e^{-ik_0 S_0} = 0. \quad (14)$$

Further, assuming the variation of A_1 as

$$A_1 = A_{10}(x,y,z)\exp[-ik_0 S_1(x,y,z)], \quad (15)$$

where A_{10} and S_1 are the real functions of space, using the paraxial ray approximation, substituting Eq. (15) into Eq. (14), and separating the real and imaginary parts of the resulting equation, the following set of equations is obtained:

$$2\frac{\partial S_1}{\partial x} + \left(\frac{\partial S_1}{\partial y}\right)^2 + \left(\frac{\partial S_1}{\partial y}\right)^2 = \frac{1}{k_0^2 A_{10}}\left(\frac{\partial^2 A_{10}}{\partial y^2}+\frac{\partial^2 A_{10}}{\partial z^2}\right) + \frac{\phi_{\text{eff}}}{\varepsilon_0}, \quad (16a)$$

where

$$\phi_{\text{eff}} = \phi(E\cdot E^*) + \frac{\omega_{p0}^2}{2\omega_0^2}\alpha A_0^2(1+\alpha A_0^2)^{-3/2}2\cos^2\phi_p$$

and

$$\frac{\partial A_{10}^2}{\partial x} + \frac{\partial A_{10}^2}{\partial y}\frac{\partial S_1}{\partial y} + \frac{\partial A_{10}^2}{\partial y}\frac{\partial S_1}{\partial y} + A_{10}^2\left(\frac{\partial^2 S_1}{\partial y^2}+\frac{\partial^2 S_1}{\partial z^2}\right) + \left[\frac{\omega_0^2}{c^2}\frac{1}{k_0}\frac{\omega_{p0}^2}{2\omega_0^2}\alpha A_0^2(1+\alpha A_0^2)^{-3/2}\sin 2\phi_p\right]A_{10}^2 = 0, \quad (16b)$$

where ϕ_p is the angle between the electric vectors of the main beam and the ripple. In writing Eqs. (16), we have expanded

$$\phi(E\cdot E^*) = \phi(E_0\cdot E_0^*) + \left.\frac{d\phi}{dE\cdot E^*}\right|_{E\cdot E^* = E_0\cdot E_0^*}(E\cdot E^* - E_0\cdot E_0^*). \quad (17)$$

The solution of Eqs. (16a) and (16b) can be written as[27]

$$A_{10}^2 = \frac{E_{100}^2}{f_1^2}\left(\frac{r}{r_{10}f_1}\right)^{2n} \exp\left(-\frac{r}{r_{10}f_1}\right)^2 \exp\left(-2\int_0^x g_i(x)dx\right),$$

$$S_1 = \frac{r^2}{2}\beta_1(x) + \phi_1(x), \tag{18}$$

$$\beta_1(x) = \frac{1}{f_1}\frac{df_1}{dx},$$

$$g_i(x) \approx \frac{1}{2}\frac{\omega_0^2}{c^2}\frac{1}{k_0}\frac{\omega_{p0}^2}{2\omega_0^2}\frac{\alpha E_{00}^2}{f_0^2(x)}\left(1 + \frac{\alpha E_{00}^2}{f_0^2(x)}\right)^{-3/2} \sin 2\phi_p,$$

where g_i and f_1 are the growth rate and the dimensionless beam width parameter of the ripple, respectively, and $\phi_1(x)$ is a constant. Substituting for A_{10} and S_1 from Eq. (18) into Eq. (16a) and expanding ϕ_{eff} around $r = r_{10}f_1 n^{1/2}$ by Taylor expansion as

$$\phi_{\text{eff}} = \phi_{\text{eff}}(r^2 = r_{10}^2 f_1^2 n) + \phi' r^2,$$

where

$$\phi' = \left.\frac{d\phi_{\text{eff}}}{dr^2}\right|_{r^2 = r_{10}^2 f_1^2 n}$$

and

$$\phi' = -\frac{1}{2}\frac{\omega_{p0}^2}{\omega_0^2 r_0^2}\alpha E_{00}^2\Bigg\{\left[1 + \alpha E_{00}^2 e^{-\left(nr_{10}^2 f_1^2/r_0^2\right)}\right]^{-3/2} \times e^{-\left(nr_{10}^2 f_1^2/r_0^2\right)} + \frac{E_{100}}{E_{00}} n^{n/2} e^{-g_i x} f_1^n \cos\phi_p e^{(-n/2)\left[1+\left(r_{10}^2 f_1^2/r_0^2\right)\right]}$$
$$\times \left\{3\alpha E_{00}^2 e^{-\left(nr_{10}^2 f_1^2/r_0^2\right)}\left[1 + \alpha E_{00}^2 e^{-\left(nr_{10}^2 f_1^2/r_0^2\right)}\right]^{-5/2} - \left[1 + \alpha E_{00}^2 e^{-\left(nr_{10}^2 f_1^2/r_0^2\right)}\right]^{-3/2}\right\} - \frac{2\cos^2\phi_p}{f_0^4} e^{-\left(nr_{10}^2 f_1^2/r_0^2 f_0^2\right)}$$
$$\times \left[\left(1 + \alpha E_{00}^2 e^{-\left(nr_{10}^2 f_1^2/r_0^2 f_0^2\right)}\right)^{-3/2} - \frac{3}{2}\alpha E_{00}^2\left[1 + \alpha E_{00}^2 e^{-\left(nr_{10}^2 f_1^2/r_0^2 f_0^2\right)}\right]^{-5/2}\right]\Bigg\}. \tag{19}$$

The following equation has been obtained for the beam width parameter of the ripple[29] after equating the coefficient of r^2:

$$\frac{d^2 f_1}{dx^2} = \frac{c^2}{\omega_0^2 \varepsilon_0 r_{10}^4 f_1^3} + \frac{\phi' f_1}{\varepsilon_0}. \tag{20}$$

Equation (20) determines the focusing/defocusing of a ripple and has the same form as the equation of self-focusing for the main beam equation (11).

III. EXCITATION OF UPPER HYBRID WAVE IN THE PRESENCE OF A LASER SPIKE

In the dynamics of the excitation of upper hybrid waves, it must be mentioned here that the contribution of ions is negligible because they only provide a static positive background, i.e., electrons in the plasma are only responsible for the excitation of upper hybrid waves. The background plasma density is modified via relativistic electron mass variation. Therefore, the amplitude of upper hybrid waves, which depends on the background electron density, gets strongly coupled to the laser beam. The magnitude of the relativistic self-focusing is modified in the presence of a ripple because it depends on the intensity of the main beam and of the ripple. Thus, the presence of the ripple must lead to a change in the modified background electron density and the excitation of the UHW is modified. In order to study the effect of the presence of the ripple on the excitation of an upper hybrid wave, we first set up the equation of the upper hybrid wave and then this nonlinear equation was solved. Following the standard method, the equation governing the upper hybrid wave in hot collisionless magnetoplasma can be written as

$$\frac{\partial^2 n}{\partial t^2} + 2\Gamma_u \frac{\partial n}{\partial t} - v_{th}^2 \nabla_n^2 - \frac{1}{\gamma_0}\frac{\omega_{p0}^2 \omega^2}{(\omega_c^2 - \omega^2)} n = 0, \tag{21}$$

where $\omega_c = eB_0/mc$ is the electron cyclotron frequency and $v_{th} = [\gamma k_B T_0/m]^{1/2}$ is the electron thermal velocity. To solve Eq. (21) for n, we follow the approach developed by Akhmanov *et al.*[26] and Sodha *et al.*[27] and express

$$n = n_0(x,y,z)\exp[i(\omega t - kx)], \tag{22}$$

where $n_0(x,y,z)$ is the complex function of its argument, and ω and k are the frequency and the propagation vector of the upper hybrid wave, respectively, related by the dispersion relation[14,33]

$$\omega^2 = \frac{\omega^2 \omega_p^2}{\omega^2 - \omega_c^2} + k^2 v_{th}^2. \tag{23}$$

For an upper hybrid wave of constant frequency ω, the propagation vector k becomes a function of the space variable on account of the modified intensity of the laser beam [Eq. (10)] and hence the modified background electron concentration. Substituting for n from Eq. (22) in Eq. (21), we get

$$[-\omega^2+2i\Gamma_u\omega]n_0-v_{th}^2\left[-k^2n_0-2ik\frac{\partial n_0}{\partial x}+\frac{\partial^2 n_0}{\partial y^2}+\frac{\partial^2 n_0}{\partial z^2}\right] - \frac{\omega_{p0}^2\omega^2}{\gamma_0(\omega_c^2-\omega^2)}n_0=0. \tag{24}$$

Furthermore, we express n_0 as

$$n_0=n_{00}(x,y,z)e^{[-iS(x,y,z)]}, \tag{25}$$

where n_{00} and S are the real functions of their arguments; S is known as the eikonal. Substituting for n_0 from Eq. (25) in Eq. (24) and separating the real and the imaginary parts, we obtain the following equations:

$$2k\frac{\partial S}{\partial x}+\left(\frac{\partial S}{\partial y}\right)^2+\left(\frac{\partial S}{\partial z}\right)^2=\frac{1}{n_{00}}\left[\frac{\partial^2 n_{00}}{\partial y^2}+\frac{\partial^2 n_{00}}{\partial z^2}\right] + \frac{1}{v_{th}^2}\left[\omega^2-k^2v_{th}^2+\frac{1}{\gamma_0}\frac{\omega^2\omega_{p0}^2}{(\omega_c^2-\omega^2)}\right] \tag{26}$$

and

$$k\frac{\partial n_{00}^2}{\partial x}+\left[\frac{\partial S}{\partial y}\frac{\partial n_{00}^2}{\partial y}+\frac{\partial S}{\partial z}\frac{\partial n_{00}^2}{\partial z}\right]+n_{00}^2\left[\frac{\partial^2 S}{\partial y^2}+\frac{\partial^2 S}{\partial z^2}\right]+\frac{2\Gamma_u\omega}{v_{th}^2}n_{00}^2 =0. \tag{27}$$

To solve the coupled equations (26) and (27), we assume the initial radial variation of density perturbation to be

$$n_{00}^2\big|_{x=0}=n_{100}^2e^{[-r^2/a_0^2]},$$

where a_0 is the half-width of the Gaussian distribution and n_{100} is the initial density associated with the plasma wave at $r=0$. The solution of Eqs. (26) and (27) can be written as

$$S=\frac{r^2}{2}\beta_u x+\phi(x), \quad \beta_u=\frac{1}{f_u}\frac{df_u}{dx}, \quad \text{and} \quad n_{00}^2=\left(\frac{n_{100}^2}{f_u^2}\right)e^{[-r^2/a_0^2f_u^2]}e^{\left[-\int_0^x 2k_i(x)dx\right]}, \tag{28}$$

where $k_i=\Gamma_{u\omega}/k(x)v_{th}^2$ is the damping factor and β_u^{-1} may be interpreted as the radius of curvature of the beam of upper hybrid waves; f_u is a dimensionless beam-width parameter. For an initially plane wave front,

$$df_u/dx=0 \quad \text{and} \quad f_u=1 \quad \text{at} \quad x=0. \tag{29}$$

The expression for f_u can be obtained by using the paraxial ray approximation under the condition $r^2 \ll a_o^2 f_u^2$. Substituting S and from n_{00}^2 Eq. (28) in Eq. (26), and equating the coefficients of r^2 on both sides, we obtain

$$\frac{d^2f_u}{dx^2}=\frac{1}{k^2a_0^4f_u^3}-\frac{1}{2}\frac{\omega^2\omega_{p0}^2}{k^2\nu_{th}^2(\omega_c^2-\omega^2)}\left\{\left[\frac{1}{r_0^2f_0^4}e^{-\left(r_{10}^2f_1^2n/r_0^2f_0^2\right)}-\frac{n^{n/2}E_{100}\cos\phi_p\exp\left(-\int_0^x g_i dx\right)}{E_{00}f_0f_1}\frac{1}{r_0^2f_0^2}e^{(-n/2)\left[1+(r_{10}^2f_1^2/r_0^2f_0^2)\right]}\right]\right.$$
$$\left.\times\left[1+\frac{\alpha E_{00^2}}{f_{0^2}}e^{-\left(r_10^2f_1^2n/r_0^2f_0^2\right)}+\frac{2E_{100}\cos\phi_p n^{\frac{n}{2}}\exp\left(-\int_0^x g_i dx\right)}{E_{00}f_0f_1}e^{(-n/2)\left[1+(r_10^2f_1^2/r_0^2f_0^2)\right)}\right]^{3/2}\right\}. \tag{30}$$

To see the effect of a laser spike and a static magnetic field on the excitation of the upper hybrid wave, we have plotted the enhancement of density perturbations associated with the upper hybrid wave with the propagation distance for different values of laser powers and the strength of the magnetic field. The following set of parameters has been used in the numerical calculations: $\omega_0=1.778\times10^{14}$ rad/s, $\omega_{p0}=0.35\omega_0$, $\omega^2=0.2\omega_0^2$, $r_0=a_0=20$ μm, $\nu_{th}=c/2$, $r_{100}=10$ μm, $n=1.5$, and $2\phi_p=3\pi/2$.

IV. RESULTS AND DISCUSSION

We have studied first the effect of a laser spike on the excitation of an upper hybrid wave by a relativistic laser beam in a hot collisionless magnetoplasma. Ripple growth/decay in the plasma is due to the coupling between the main laser beam and the ripple. The growth rate (g_i) of the ripple [Eq. (18)] depends on the effective intensity of the main beam in the plasma, electron density in the plasma, frequency of the laser beam, and phase angle ϕ_p. It has been observed that the ripple will grow only when $\sin 2\phi_p$ is negative in Eq. (18). Figure 1 shows the variation of the growth rate (g_i) with the distance of propagation at different laser powers. The growth rate of the ripple decreases continuously when the power of the beam is increased.

For an initially plane wave front of the laser beam, the initial conditions used here are $df_1/dx=0$ and $f_1=1$ at $x=0$. Figures 2 and 3, respectively, illustrate the variation of the beam-width parameter of the main beam (f_0) [Eq. (11)] and the ripple (f_1) [Eq. (20)] with the distance of propagation at different laser powers. The periodic structure is a signature of beam propagation in a nonlinear media with a power in excess of the critical power for self-focusing. The power of the beam and the phase difference between the electric vector of the main beam and the ripple are found to change the self-focusing of the ripple significantly. The growth rate (g_i)

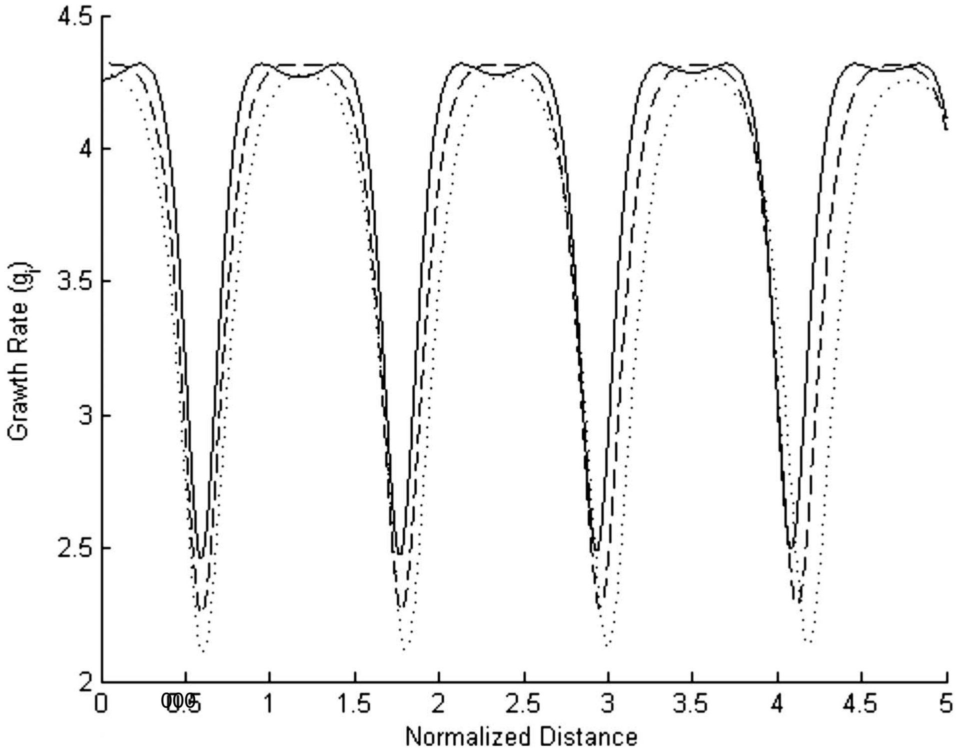

FIG. 1. Variation of the growth rate (g_i) of the ripple with the normalized distance of propagation $(\xi = xc/\omega_0 r_0^2)$ for different laser powers. Solid, dotted, and dashed lines are for $\alpha E_{00}^2 = 1.25$, 1.75, and 2.25, respectively.

contributes significantly to relativistic self-focusing of a rippled laser beam in a plasma. The beam width of the ripple decreases with the distance of propagation when the power of the beam is increased (Fig. 3). It has been observed that a small spike on the axis of the main beam grows very rapidly with distance of propagation as compared with self-focusing of the main beam.

Figure 4 depicts the variation of normalized axial intensity of the ripple with propagation distance for different values of laser powers and fixed n and ϕ_p when the main beam is propagating in the self-trapping mode $(f_0 = 1)$. When $\sin 2\phi_p = 3\pi/2$, the intensity of the ripple increases first and oscillates with the distance of propagation because the growth rate affects significantly the intensity dynamics of the

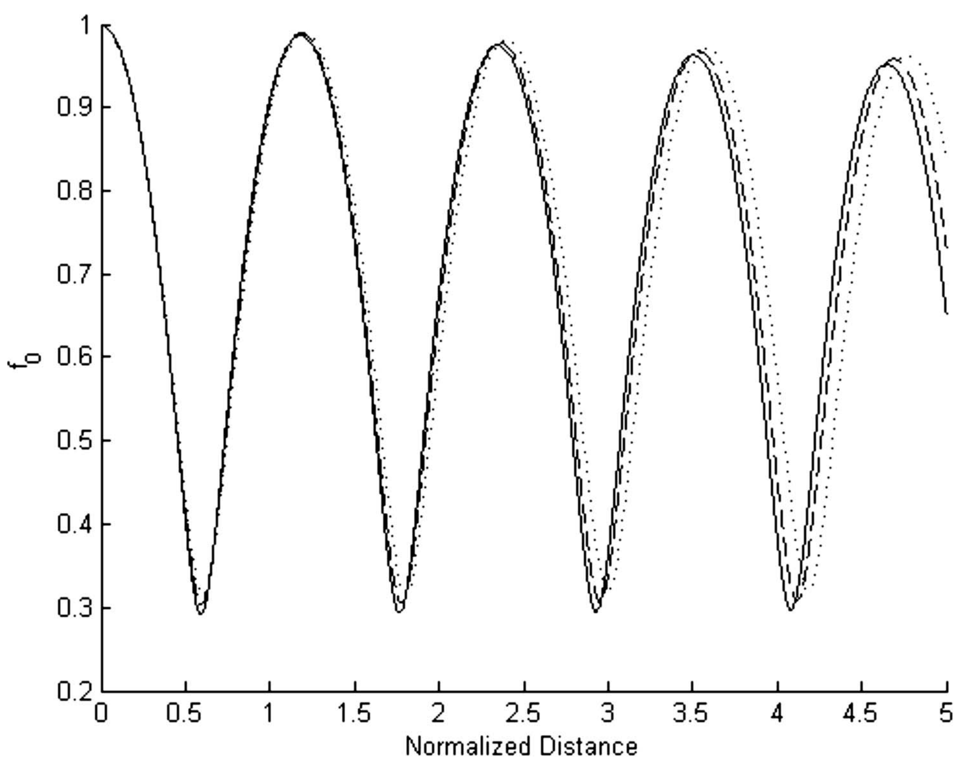

FIG. 2. Variation of the dimensionless beam width parameter (f_0) of a pump laser beam with the normalized distance of propagation $(\xi = xc/\omega_0 r_0^2)$ for different laser powers. Solid, dotted, and dashed lines are for $\alpha E_{00}^2 = 1.25$, 1.75, and 2.25, respectively.

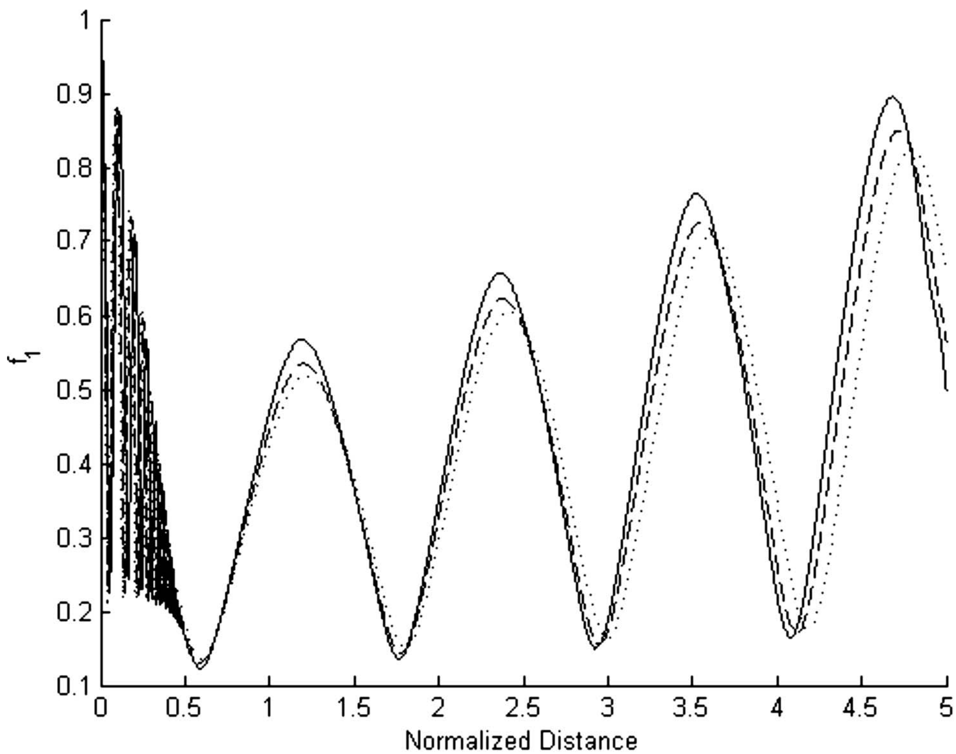

FIG. 3. Variation of the dimensionless beam width parameter (f_1) of the ripple with the normalized distance of propagation $(\xi = xc/\omega_0 r_0^2)$ for different laser powers. Solid, dotted, and dashed lines are for $\alpha E_{00}^2 = 1.25$, 1.75, and 2.25, respectively.

ripple. The increase in intensity of the ripple also depends on the beam width parameter (f_1) of the ripple and the position of the ripple (n). When the power of the laser is increased, the axial intensity of the ripple is decreased due to the combined effect of the growth rate and the beam width parameter (f_1) of the ripple.

The effect of the initial power of the rippled laser beam and the strength of magnetic field on the excitation of the upper hybrid wave have been depicted in Figs. 5–8, respectively. Figures 5 and 6 show the variation of the bandwidth of the upper hybrid wave (f_u) [Eq. (30)] and enhancement in the density perturbation (n_{00}^2/n_{100}^2) [Eq. (28)] in the presence of laser spike with the propagation distance for different laser powers and fixed ω_c/ω. It is obvious from the graphs that the beam width and density perturbation of the upper hybrid wave are significantly affected by the growth rate and pow-

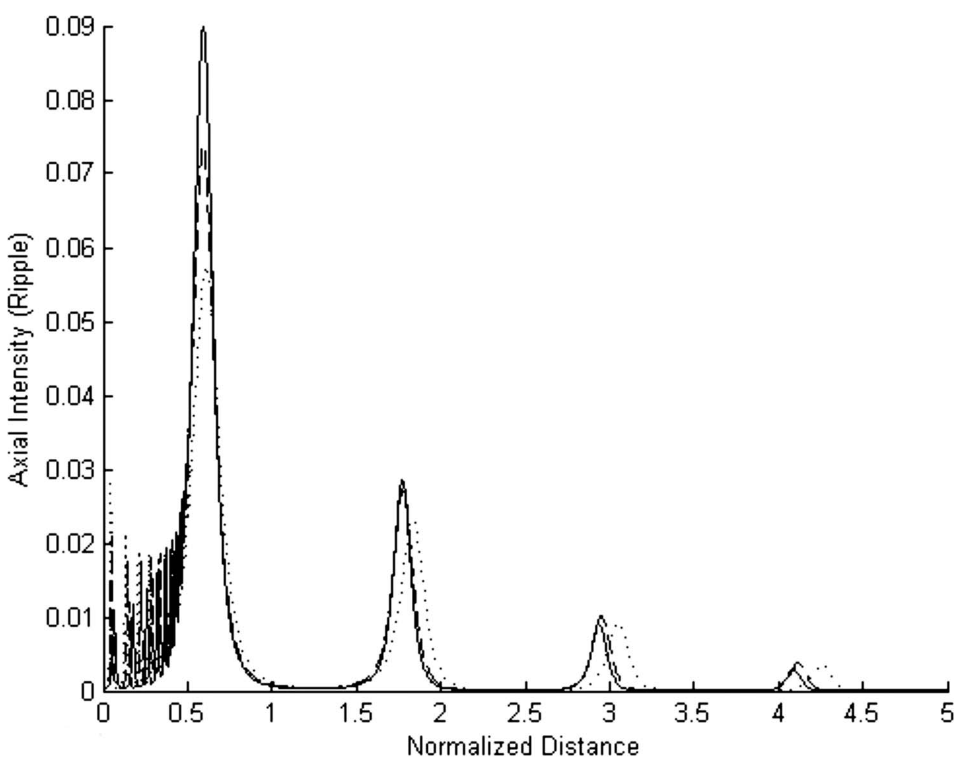

FIG. 4. Variation of the normalized axial intensity of the ripple with the normalized distance of propagation $(\xi = xc/\omega_0 r_0^2)$ for different laser powers. Solid, dotted, and dashed lines are for $\alpha E_{00}^2 = 1.25$, 1.75, and 2.25, respectively.

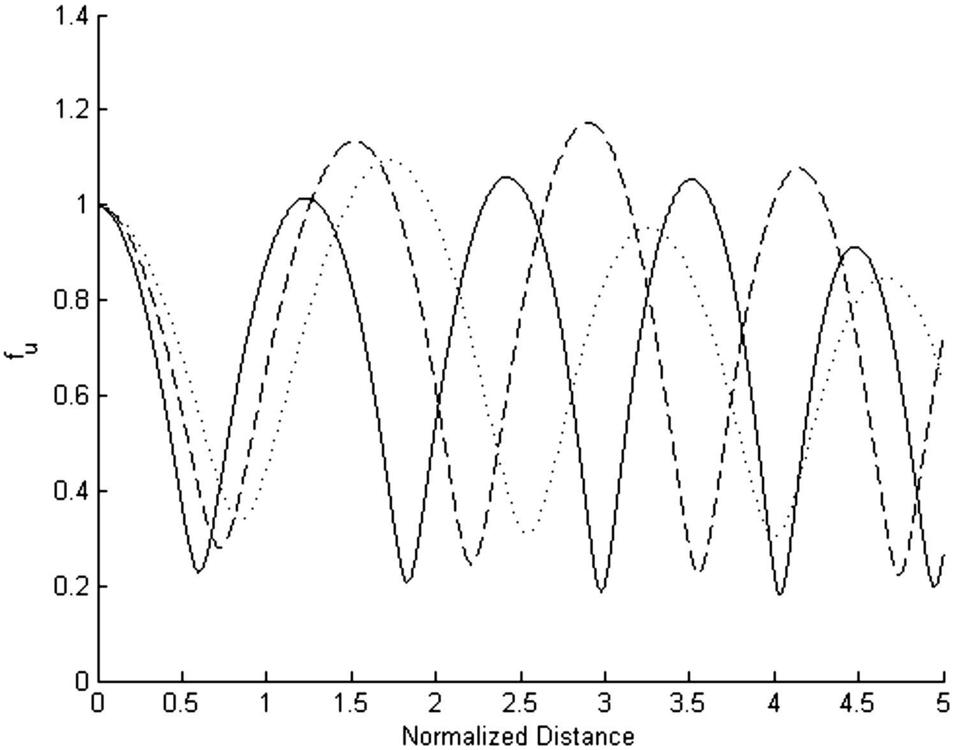

FIG. 5. Variation of the dimensionless beam width parameter of the upper hybrid wave (f_p) with the normalized distance of propagation $(\xi = xc/\omega_0 r_0^2)$ for different laser powers with fixed $\omega_c/\omega_0 = 0.5$. Solid, dotted, and dashed lines are for $\alpha E_{00}^2 = 1.25$, 1.75, and 2.25, respectively.

ers of the laser beam. When the power of the beam is increased, the bandwidth of the upper hybrid wave increases and shows oscillatory character due to self-focusing of the main beam and the ripple, which attains a low level as the distance of propagation increases. In the presence of a laser spike, initially a small spike grows during density perturbation and then the amplitude of the upper hybrid wave increases with the propagation distance. Figure 6 displays that amplitude of the density perturbation associated with upper hybrid wave decreases when the power of the beam is increased, however the density perturbation profile is almost the same. This shows that the amplitude of the density perturbation depends on the growth rate of the ripple and laser power.

To study the effect of the strength of the magnetic field on the excitation of the upper hybrid wave, we have plotted

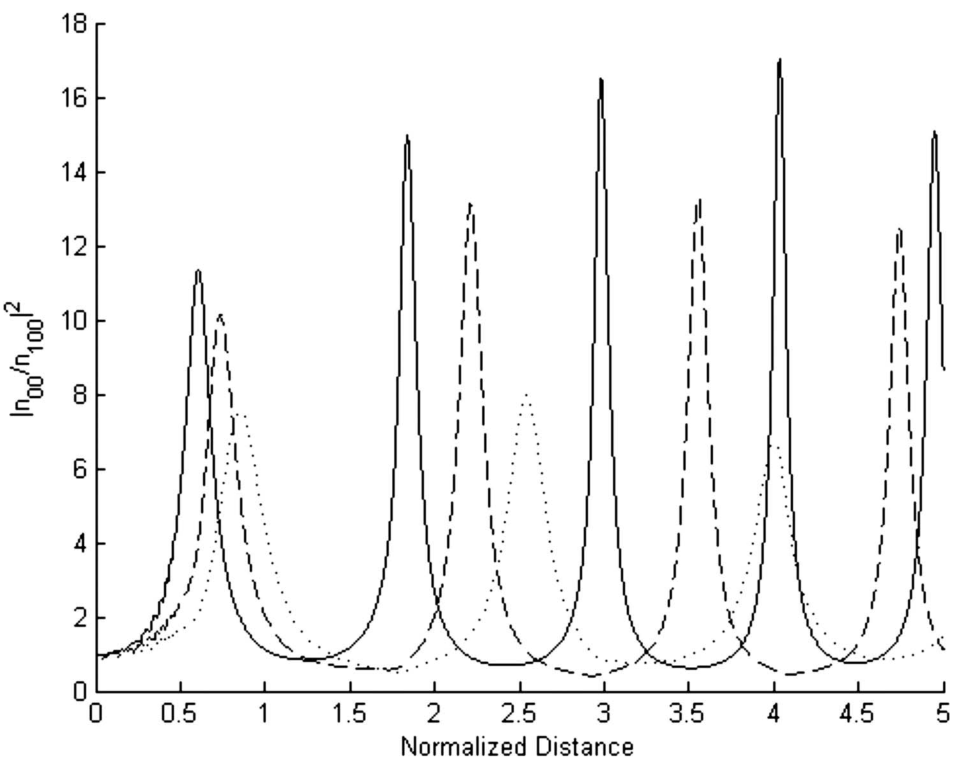

FIG. 6. Variation of the density perturbation associated with the upper hybrid wave $(n_{00}/n_{100})^2$ with the normalized distance of propagation $(\xi = xc/\omega_0 r_0^2)$ for different values of with fixed $\omega_c/\omega_0 = 0.5$. Solid, dotted, and dashed lines are for $\alpha E_{00}^2 = 1.25$, 1.75, and 2.25, respectively.

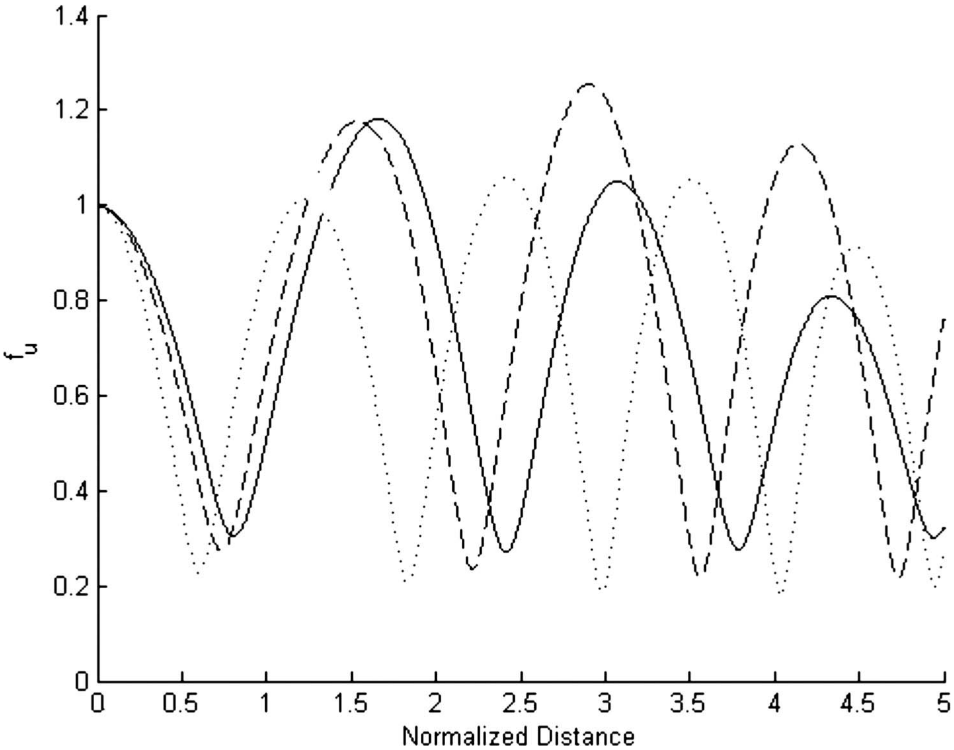

FIG. 7. Variation of the dimensionless beam width parameter of the upper hybrid wave (f_p) with the normalized distance of propagation $(\xi = xc/\omega_0 r_0^2)$ for different ω_c/ω_0 with fixed $\alpha E_{00}^2 = 1.75$. Solid, dotted, and dashed lines are for $\omega_c/\omega_0 = 0.3$, 0.5, and 0.7, respectively.

the beam width of the excited upper hybrid wave and density perturbation versus propagation distance for different ω_c/ω, when the initial power of the pump wave is between two critical powers P_{cr1} and P_{cr2} in Figs. 7 and 8, respectively. It is clear from Fig. 7 that the focusing/defocusing behavior of the upper hybrid wave is critically dependent on the strength of the magnetic field. The excited upper hybrid wave exhibits oscillatory focusing, which again shifts its maxima and minima by changing the strength of the magnetic field. However, when $\omega_c/\omega_0 = 0.5$, the bandwidth of the excited upper hybrid wave attains a maximum value after propagating a certain distance. Figure 8 displays the variation of the density perturbation associated with the upper hybrid wave with propagation distance. We observe that the magnitude of the density perturbation associated with the upper hybrid wave is decreased when the strength of the magnetic field is in-

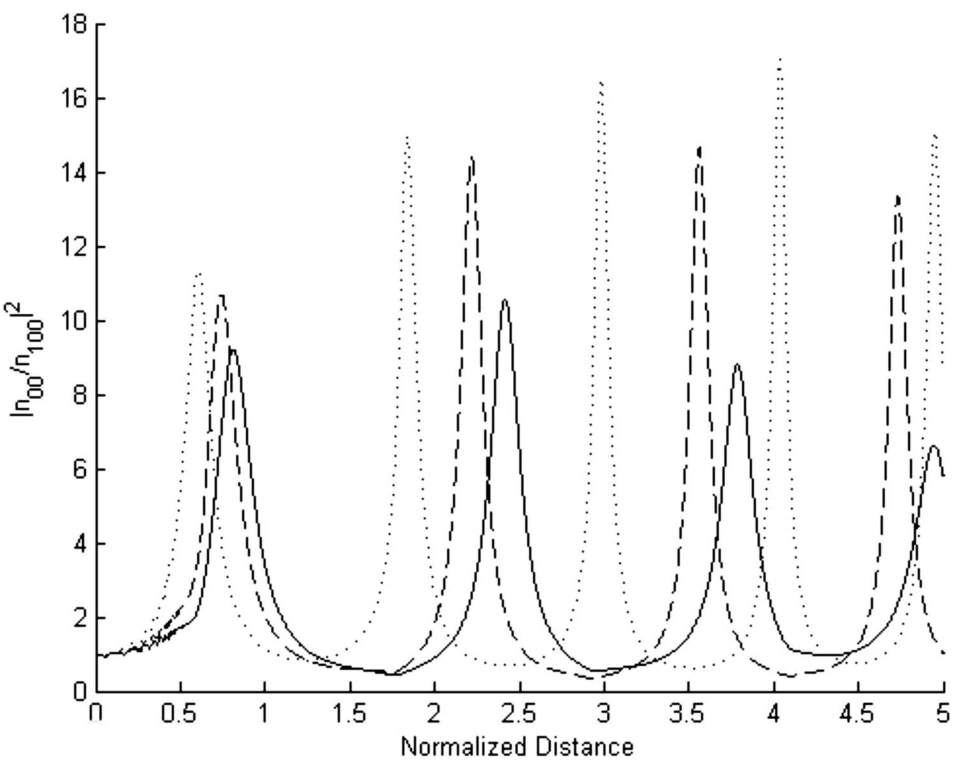

FIG. 8. Variation of the density perturbation associated with the upper hybrid wave $(n_{00}/n_{100})^2$ with the normalized distance of propagation $(\xi = xc/\omega_0 r_0^2)$ for different ω_c/ω_0 with fixed $\alpha E_{00}^2 = 1.75$. Solid, dotted, and dashed lines are for $\omega_c/\omega_0 = 0.3$, 0.5, and 0.7, respectively.

creased. The maximum magnitude is dependent on the focusing of the upper hybrid wave. The focusing/defocusing nature and density perturbation associated with the excited upper hybrid wave also depends on various parameters such as the growth rate of the ripple superimposed on the main beam, the position of the ripple, the angle between the electric vectors of the main beam and the ripple, the laser power, and the modified background density of the electrons via the relativistic mass variation. These parameters control the coupling of the upper hybrid wave with the pump wave, which affects the excitation of the upper hybrid wave significantly.

In conclusion, the results show that the rippled laser beam and static magnetic field significantly affect the dynamics of the excitation of the upper hybrid wave. The focusing nature of the upper hybrid wave is highly dependent on the initial power of the laser beam, the growth rate of the ripple superimposed on the main laser beam, and the strength of the magnetic field. This work shows the real dynamics of the excitation of the upper hybrid wave at relativistic power in magnetoplasma because of the presence of the ripple superimposed on the main beam. These results should find applications in the heating of plasmas near the upper hybrid frequency (laser-induced fusion) and particle acceleration. Besides this, the present model provides some insight into the coupling physics of the laser plasma interaction.

ACKNOWLEDGMENTS

This work is supported by the Department of Science & Technology (DST), New Delhi, India.

[1]W. L. Kruer, *The Physics of Laser Plasma Interaction* (Addison-Wesley, New York, 1988), p. 27.
[2]A. Modena, Z. Najmudin, A. E. Dangor, C. E. Clayton, K. A. Marsh, C. Joshi, V. Malka, C. B. Darrow, C. Danson, D. Neely, and F. N. Walsh, Nature **377**, 606 (1995).
[3]J. S. Wurtele, Phys. Today **47**(7), 33 (1994).
[4]M. J. Herbst, C. E. Clayton, and F. F. Chen, Phys. Rev. Lett. **43**, 1591 (1979).
[5]Y. Kato, K. Mima, N. Miyaraga, S. Arinaga, Y. Kitagawa, M. Nikatusuka, and C. Yamanaka, Phys. Rev. Lett. **53**, 1057 (1984).
[6]R. H. Lehmberg and S. Obenschain, Opt. Commun. **46**, 27 (1983); R. H. Lehmberg, A. J. Schmitt, and S. E. Bodner, J. Appl. Phys. **62**, 2680 (1987).
[7]S. Spupsky, R. W. Short, T. Kessler, R. S. Craxton, S. Letzring, and J. M. Soures, J. Appl. Phys. **66**, 3456 (1987).
[8]A. B. Borisov, O. B. Shiryaev, A. McPherson, K. Boyer, and C. K. Rhodes, Plasma Phys. Controlled Fusion **37**, 569 (1995).
[9]A. V. Brantov, V. Yu. Bychenkov, V. T. Tikhonchuk, W. Rozmus, and V. K. Senecha, Phys. Plasmas **6**, 3002 (1999).
[10]P. K. Kaw, G. Schmidt, and T. Wilcox, Phys. Fluids **16**, 1522 (1973).
[11]D. P. Singh, R. P. Sharma, and S. C. Kaushik, J. Phys. D **12**, 83 (1979).
[12]H. D. Pandey and V. K. Tripathi, Phys. Fluids B **2**, 1221 (1990).
[13]S. Sartang, R. G. Evans, and W. T. Toner, J. Phys. D **16**, 955 (1983).
[14]S. Wilks, P. E. Young, J. Hammer, M. Tabak, and W. L. Kruer, Phys. Rev. Lett. **73**, 2994 (1994).
[15]A. J. Schmitt, Phys. Fluids **31**, 3079 (1988).
[16]C. Ren, R. G. Hemker, R. A. Fonseca, B. J. Duda, and W. B. Mori, Phys. Rev. Lett. **85**, 2124 (2000).
[17]K. A. Brueckner and S. Jorna, Rev. Mod. Phys. **46**, 325 (1974); M. Kristiansen and M. O. Hagler, Nucl. Fusion **16**, 999 (1976).
[18]T. H. Stix, Phys. Rev. Lett. **15**, 878 (1965).
[19]S. R. Seshadri, J. Appl. Phys. **45**, 4826 (1974).
[20]N. T. Hung, Plasma Phys. **17**, 633 (1975).
[21]J. J. Schuss and J. C. Hosea, Phys. Fluids **18**, 727 (1975).
[22]K. F. Lee, Phys. Fluids **17**, 1220 (1974); Phys. Lett. **47A**, 257 (1974).
[23]N. A. Krall and A. W. Trivelpiece, *Principles of Plasma Physics* (McGraw-Hill, New York, 1973), p. 197.
[24]V. B. Krasovitskiy, V. A. Turikov, and V. I. Sotnikov, Phys. Plasmas **14**, 092108 (2007).
[25]V. B. Krasovitskiy, V. G. Dorofeenko, V. A. Turikov, and V. I. Sotnikov, Plasma Phys. Rep. **32**, 26 (2006).
[26]V. I. Sotnikov, Y. Sentoku, and V. B. Krasovitskiy, Phys. Plasmas **12**, 082107 (2005).
[27]M. S. Sodha, D. P. Tewari, B. L. Patheja, and R. P. Sharma, J. Plasma Phys. **21**, 267 (1979).
[28]C. Grebogi and C. C. Liu, J. Plasma Phys. **23**, 147 (1980).
[29]M. S. Sodha, T. Singh, D. P. Singh, and R. P. Sharma, Phys. Fluids **24**, 914 (1981).
[30]S. A. Akamanov, A. P. Sukhorukov, and R. V. Khokhiov, Sov. Phys. Usp. **10**, 609 (1968).
[31]M. S. Sodha, A. K. Ghatak, and V. K. Tripathi, Prog. Opt. **13**, 169 (1976).
[32]G. Purohit, H. D. Pandey, S. T. Mahmoud, and R. P. Sharma, J. Plasma Phys. **70**, 25 (2004).
[33]F. F. Chen, *Introduction to Plasma Physics and Controlled Fusion* (Plenum, New York, 1984).